Available online at www.sciencedirect.com
ScienceDirect
Journal of Sound and Vibration 322 (2009) 941–953
JOURNAL OF SOUND AND VIBRATION
www.elsevier.com/locate/jsvi

Nonlinear dynamic behaviour of a preloaded thin sandwich plate incorporating visco-hyperelastic layers

H. Gacem[a,b,*], Y. Chevalier[a], J.L. Dion[a], M. Soula[b], B. Rezgui[b]

[a] *Laboratoire d'Ingénierie des Systèmes Mécaniques et des Matériaux, Institut Superieur de Mécanique de Paris, 3 rue Fernand Hainaut, 93407 Saint Ouen Cedex, Paris, France*

[b] *Unité de Recherche Génie des Matériaux, Ecole Nationale d'Ingénieurs de Tunis, BP 37 Le Belvédère Tunis, Tunisia*

Received 23 May 2008; received in revised form 21 October 2008; accepted 12 November 2008
Handling Editor: C.L. Morfey
Available online 19 January 2009

Abstract

The nonlinear dynamic behaviour of preloaded traditional multilayer plates incorporating visco-hyperelastic materials is investigated. The visco-hyperelastic material was confined between stiff layers and worked as a damping layer. The full structure is submitted to shear vibrations under a compression preload. We present herein a nonlinear model describing the tangent dynamic shear modulus as function of both preload and frequency. A Navier approach is used to calculate the stress and the deformation fields which are written by a transfer matrix formulation. The dynamic shear modulus for elastomers is expressed by a nonlinear visco-hyperelastic model based on a deformation energy density. The effects of the elastomer's nonlinear behaviour, the frequency and the preload on the structure's overall dynamic shear modulus is the main object of this study. Verification of the model is performed on visco-hyperelastic multilayer through a series of dynamic shear tests under various compression preload levels. A comparison with both finite element calculations and discreet models is discussed.

1. Introduction

The ever increasing use of composite materials, in particular laminate structures, in all types of engineering systems has given a strong impetus to the development of composite material systems as well as to the analysis and design of structural components over the last two decades. The subject of composite materials is truly an interdisciplinary area where chemists, materials scientists, mechanical engineers and structural engineers contribute to the overall product. Research published on composite materials falls into three categories: materials science [1], mechanics [2] and design [3].

The present study belongs to the second category which concerns visco-hyperelastic multilayers. In order to dampen vibration and thus avoid serious damage, viscoelastic materials, which have substantial energy absorption abilities, can be incorporated into the structural system. The use of multilayer absorbers has

*Corresponding author at: Laboratoire d'Ingénierie des Systèmes Mécaniques et des Matériaux, Institut Superieur de Mécanique de Paris, 3 rue Fernand Hainaut, 93407 Saint Ouen Cedex, Paris, France. Tel.: +33 6 69 74 92 75.
E-mail address: gacem_hatem@yahoo.fr (H. Gacem).

0022-460X/$ - see front matter
doi:10.1016/j.jsv.2008.11.040

become increasingly important in vibration, especially in damping vibration and noise of brake systems. To ensure the vibration and acoustic absorption of the multilayer absorber, selecting appropriate shock-absorbent materials and choosing an optimal geometric design for the structures have become major concerns.

Different methods have been developed for modelling the behaviour of viscoelastic multilayer structures. Each is valid for specific materials and particular loads. For example, consider the plate with visco-hyperelastic layers sandwiched between several stiff layers which was first introduced by Swallow [4] as early as 1939. Since then a number of investigations on the design formulations for thin multilayer sandwich plates have been carried out by various researchers. Kerwin [5] suggested a complete and simplified formula for estimating loss factors as a function of the wavelength refraction, the thickness of the constraining layer and the plate's elastic modulus. On the basis of the foregoing research, Ungar and Kerwin [6] were able to correlate the loss factors to energy concepts. Di Taranto [7] derived a sixth-order complex homogeneous differential equation for a free vibrating finite-length sandwich beam. Di Taranto and Blasingame [8] continued Kerwin's work and published a damping-frequency dependence function for selected laminated beams. Mead and Markus [9] pursued the previous studies and developed a sixth-order differential equation formulated in terms of transverse displacement for the forced vibration of sandwich beams under specific "damped normal loadings".

A simple numerical method using a one-dimensional approximation is presented by Fujii [10] for analysing the dynamic response of adhesively bonded sandwich beams in which the visco-elastic characteristics of the adhesive damping layer are represented by a generalized Maxwell model. Likewise, Njilie et al. [11] developed a finite element model for sandwich plates by considering them as a superposition of linear elastic plates. In their work, damping is predicted through the evaluation of the loss factor introduced by Ungar and Kerwin [6] which is a function of material and geometric properties of the structure.

Yuh-Chun and Shyh-Chin [12] presented a mathematical model for the vibrations of three-layer structures with viscoelastic cores for which the dependent model is adopted for the dynamic modulus. As presented in the results of experimental testing for the visco-hyperelastic multilayers [13,14], nonlinear behaviour was observed in the stress–strain relationships, particularly during higher frequency loading tests. Therefore, it is not suitable to use traditional models to describe this nonlinear behaviour. To overcome this limitation, certain analytical nonlinear models are required. Hence, an analytical nonlinear model, which can accurately describe the mechanical behaviour of multilayer sandwich beams with viscoelastic layers, was developed by Lee and Tsai [15]. Hence, a finite element formulation combined with a new material model has been developed by Lee [16] for multilayer beams incorporating viscoelastic material having nonlinear behaviour. In the work of this latter, a nonlinear dynamic analysis as a function of time was carried out for a multilayered structure subjected to dynamic loads. As part of the effort to carry out comprehensive dynamical analysis of visco-hyperelastic composite structures, we herein develop an analytical nonlinear model to evaluate both frequency and preload dependent behaviour for thin visco-hyperelastic multilayer plates. These plates contain damping devices, submitted to shear vibration under compression preload. The developed model is based on a linearization procedure involving a finite static deformation which is a compression preload. The case of dynamic shear under shear preload is presented in the work of Saad et al. [17,18], in which the virtual work principle is used to calculate the tangent shear modulus. In our approach, we first use classical linear elasticity to derive the model frequency dependence and next visco-hyperelasticity to introduce the nonlinearity effect of elastomer layers. It is the purpose of this study to analyse the effect of nonlinear material on the global multilayer dynamic behaviour [19]. Verification of the model is performed on multilayer through a series of dynamic shear tests under various compression preload levels. A comparison with both finite element calculations and discreet models is presented.

2. Theory

2.1. Analytical solution for compression preloaded multilayer submitted to shear

Consider a multilayer composed of five layers composed of elastomer and steel disposed as shown in Fig. 1.

We suppose that the top face of structure (at $z = h$) is submitted to a vertical compression preload $\mathbf{F}_0$ ($\mathbf{F}_0 = F_0\mathbf{Z}$), while simultaneously subjected to a transverse harmonic shear in the second direction ($\mathbf{Y}$). The bottom face is adjusted into the surrounding base.

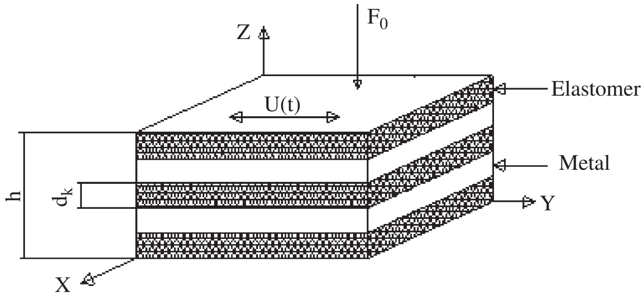

Fig. 1. Elastomer/steel multilayer submitted to compression preload and dynamic shear. d_k denotes the thickness of the kth layer and h is the overall thickness ($h = 0.94$ mm; $d_1 = d_3 = 0.12$ mm; $d_5 = 0.14$ mm; $d_2 = d_4 = 0.28$ mm).

The behaviour is considered in the case of classical linear elasticity. We define a field displacement as follows:

$$\mathbf{U}(z,t) = f(z)\sin(\omega t)\mathbf{Y} + g(z)\mathbf{Z} \tag{1}$$

where $f(z)$ and $g(z)$ are unknown functions ($g(z)$ characterizes the preload). ω is the applied circular frequency. t denotes the time. z is the global third coordinate.

Accordingly, we derive the deformation and the stress tensors in the following forms:

$$\boldsymbol{\sigma} = \begin{bmatrix} \sigma_{11} & & \text{SYM} \\ 0 & \sigma_{22} = \sigma_{11} & \\ 0 & \tau & \sigma_{33} \end{bmatrix}; \quad \boldsymbol{\varepsilon} = \begin{bmatrix} 0 & & \text{SYM} \\ 0 & 0 & \\ 0 & \varepsilon_{32} & \varepsilon_{33} \end{bmatrix} \tag{2}$$

where indices 1, 2 and 3 correspond, respectively, to X, Y and Z direction of the reference coordinate system (Fig. 1).

By applying the equilibrium equation, we obtain the following solutions for the unknown functions f and g in each kth layer:

$$\begin{cases} f_k(z) = A_k\,\mathrm{e}^{\mathrm{i}q_k z} + B_k\,\mathrm{e}^{-\mathrm{i}q_k z} \\ g_k(z) = C_k z + D_k \end{cases} \tag{3}$$

where

$$q_k^2 = \frac{\rho_k w^2}{\mu_k}$$

ρ_k and μ_k are, respectively, the material density and the shear modulus for the kth layer, ω is the angular frequency. A_k, B_k, C_k and D_k are constants which are determined using the limit conditions. $\mathrm{i}^2 = -1$.

We derive the following expressions of the stress and the displacement fields in each kth layer:

$$\begin{cases} \sigma_{11}^{(k)} = \sigma_{22}^{(k)} = \lambda_k C_k \\ \sigma_{33}^{(k)} = (2\mu_k + \lambda_k) C_k \\ \tau^{(k)}(z,t) = \mathrm{i}\mu_k q_k \sin(wt)(A_k\,\mathrm{e}^{\mathrm{i}q_k z} - B_k\,\mathrm{e}^{-\mathrm{i}q_k z}) \end{cases} \tag{4}$$

$$\begin{cases} U_y^{(k)}(z,t) = \sin(wt)(A_k\,\mathrm{e}^{\mathrm{i}q_k z} + B_k\,\mathrm{e}^{-\mathrm{i}q_k z}) \\ U_z^{(k)}(z) = C_k z + D_k \end{cases} \tag{5}$$

where λ_k is the kth layer's "Lame" coefficient.

2.2. Transfer matrix formulation

Eqs. (4) and (5) for the transverse fields of stress and displacement can be written using a matrix transfer relation as follows

$$\mathbf{L}^{(k)}(d_k) = \boldsymbol{\alpha}_k \mathbf{L}^{(k-1)}(d_{k-1}) \tag{6}$$

where

$$\mathbf{L}^{(k)}(d_k) = \begin{pmatrix} U_y^{(k)}(d_k) \\ \tau^{(k)}(d_k) \end{pmatrix}; \quad \boldsymbol{\alpha}_k = \begin{bmatrix} \cos(q_k d_k) & \dfrac{\sin(q_k d_k)}{\mu_k q_k} \\ -\mu_k q_k \sin(q_k d_k) & \cos(q_k d_k) \end{bmatrix} \tag{7}$$

Using Eq. (6), the displacement and the stress fields in the top layer (number n) and in the bottom layer (number 1) are related as

$$\mathbf{L}^{(n)}(d_n) = \boldsymbol{\alpha} \mathbf{L}^{(1)}(0) \tag{8}$$

where

$$\mathbf{L}^{(n)}(d_n) = \begin{pmatrix} U_y^{(n)}(d_n) \\ \tau^{(n)}(d_n) \end{pmatrix}; \quad \mathbf{L}^{(1)}(0) = \begin{pmatrix} U_y^{(1)}(0) = 0 \\ \tau^{(1)}(0) \end{pmatrix} \tag{9}$$

and

$$\boldsymbol{\alpha} = \boldsymbol{\alpha}_n, \ldots, \boldsymbol{\alpha}_1 \tag{10}$$

For the displacement and the stress fields of compression, we can obtain a similar relation.

Using Eq. (8), the global shear modulus of the structure can be obtained as follows:

$$\mu = h \frac{\boldsymbol{\alpha}_{22}}{\boldsymbol{\alpha}_{12}} \tag{11}$$

h is the structure thickness.

2.3. Influence of nonlinear visco-hyperelastic behaviour of elastomer layers

In this section, we are interested in studying the influence of the nonlinear visco-hyperelastic effect of elastomer layers on the dynamic behaviour of the structure. We decompose the loads into a separate a compression preload $\mathbf{F}_0$ superimposed on a shear $\mathbf{U}(t)$ characterized by the shear angle $\beta(t)$ (Fig. 2).

Let us consider (X, Y, Z) the coordinates of a point M in a nonloaded configuration. (x_1, y_1, z_1) the new coordinates after compression. (x, y, z) the final coordinates after shear.

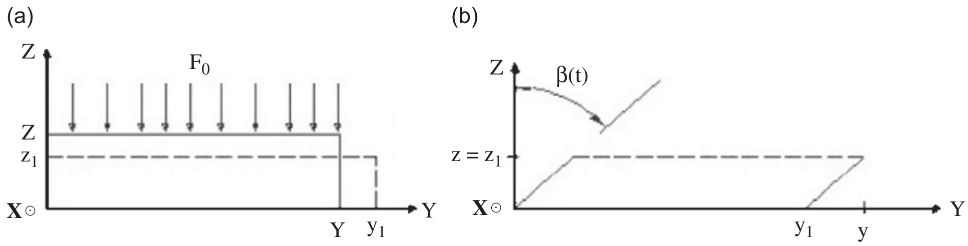

Fig. 2. Superposition of loads: (a) static compression preload and (b) dynamic shear.

By assuming incompressible transformation, we have

$$\begin{cases} x_1 = \dfrac{1}{\sqrt{\chi}}X \\ y_1 = \dfrac{1}{\sqrt{\chi}}Y \\ z_1 = \chi Z \end{cases} \quad \text{and} \quad \begin{cases} x = x_1 \\ y = y_1 + \gamma z_1 \\ z = z_1 \end{cases} \Rightarrow \begin{cases} x = \dfrac{1}{\sqrt{\chi}}X \\ y = \dfrac{1}{\sqrt{\chi}}Y + \gamma\chi Z \\ z = \chi Z \end{cases} \tag{12}$$

where χ and γ are, respectively, the compression elongation and the shear angle tangent which are assumed to be constant in the specimen. Relation (12) presents a coupling between preload and shear deformations.

The corresponding left-hand Cauchy Green dilatation tensor $\mathbf{B}$ is written as follows:

$$\mathbf{B} = \begin{bmatrix} \frac{1}{\chi} & & \text{SYM} \\ 0 & \frac{1}{\chi} + (\chi\gamma)^2 & \\ 0 & \chi^2\gamma & \chi^2 \end{bmatrix} \tag{13}$$

Using the first and the second thermodynamic principles, the Cauchy stress tensor $\boldsymbol{\sigma}$ is derived from the energy density W as follows [20]:

$$\boldsymbol{\sigma} = 2\left[\frac{\partial W}{\partial I_1} + I_1 \frac{\partial W}{\partial I_2}\right]\mathbf{B} - 2\frac{\partial W}{\partial I_2}\mathbf{B}^2 + p\boldsymbol{\delta} \tag{14}$$

where $\boldsymbol{\delta}$ is the unity tensor and p is the hydraustatic pressure. I_1 and I_2 are the first and the second invariants of the left-hand Cauchy Green dilatation tensor $\mathbf{B}$.

The relaxation tangent tensor $\mathbf{R}$ is expressed as [21]:

$$R_{ijkl} = \frac{\partial(J\sigma_{ij})}{\partial F_{kp}} F_{lp} \tag{15}$$

where $\mathbf{F}$ is the gradient transformation tensor. $J = \det(\mathbf{F})$. R_{ijkl} is the $(ijkl)$ component of $\mathbf{R}$. Using Eq. (15), we deduce the tangent shear modulus, which is the component R_{2323} of $\mathbf{R}$, in the case of harmonic shear under compression preload:

$$R_{2323} = \frac{\partial(J\sigma_{23})}{\partial F_{23}} F_{33} \tag{16}$$

By writing $\mathbf{B}$ as function of $\mathbf{F}$ and using Eqs. (14) and (16), we deduce the tangent shear modulus R_{2323} as follows:

$$R_{2333} = Q_1 \frac{\partial W}{\partial I_1} + Q_2 \frac{\partial W}{\partial I_2} + Q_{11} \frac{\partial^2 W}{\partial I_1^2} + Q_{22} \frac{\partial^2 W}{\partial I_2^2} + Q_{12} \frac{\partial^2 W}{\partial I_1 \partial I_2} \tag{17}$$

where

$$\begin{cases} Q_1 = 2F_{33}^2 \\ Q_2 = 2F_{33}^2[F_{11}^2 + F_{22}^2 + F_{33}^2 + 3F_{23}^2 - 2F_{23}F_{33}] \\ Q_{11} = 4F_{33}^2 F_{23}^2 \\ Q_{22} = 4F_{11}^2 F_{33}^2 F_{23}^3 [F_{11}^2 + F_{22}^2 + F_{33}^2 + F_{23}^2 - F_{23}F_{33}] \\ Q_{12} = 4F_{33}^2 F_{23}^2 [2F_{11}^2 + F_{22}^2 + F_{33}^2 + F_{23}^2 - F_{23}F_{33}] \end{cases} \tag{18}$$

The Q_i and Q_{ij} can be written as functions of both elongation of compression preload and the shear angle tangent:

$$\begin{cases} Q_1 = 2\chi^2 \\ Q_2 = 2\chi[2 + \chi^3(1 + 3\gamma^2 - 2\gamma)] \\ Q_{11} = 4\gamma^2\chi^4 \\ Q_{22} = 4\gamma^2\chi^2[2 + \chi^3 + \gamma^2\chi^3(1 - \chi^2)] \\ Q_{12} = 4\gamma^2\chi^3[3 + \chi^3(1 + \gamma^2 - \gamma)] \end{cases} \tag{19}$$

2.4. Gent–Thomas energy function

The Gent–Thomas energy function can characterize correctly the hyperelastic behaviour of elastomers and has a simple expression which is written as [22]

$$W = Ag_1(t)(I_1 - 3) + Bg_2(t)\ln\left(\frac{I_2}{3}\right) \tag{20}$$

where A and B are two material constants. $g_1(t)$ and $g_2(t)$ are two functions of time characterizing visco-elasticity.

In this case, using Eq. (17), the tangent shear modulus can be written as

$$R_{2323} = AQ_1g_1(t) + B\left[\frac{Q_2}{I_2} - \frac{Q_{22}}{I_2^2}\right]g_2(t) \tag{21}$$

The dynamic shear modulus under compression preload is function of three variables: the compression elongation χ, the shear γ and the time t. Hence, the tangent shear modulus is given by

$$R_{2323}(\chi, t) = \lim_{\gamma \to 0}[R_{2323}(\chi, \gamma, t)] \tag{22}$$

From Eqs. (21) and (22), we deduce the tangent shear modulus:

$$R_{2323}(\chi, t) = 2A\chi^2 g_1(t) + 2B\frac{\chi^3(2 + \chi^3)}{1 + 2\chi^3}g_2(t) \tag{23}$$

According to Eq. (23), the tangent dynamic shear modulus is written in the frequency domain as

$$\tilde{R}_{2323}(\chi, \omega) = 2A\chi^2\tilde{g}_1(\omega) + 2B\frac{\chi^3(2 + \chi^3)}{1 + 2\chi^3}\tilde{g}_2(\omega) \tag{24}$$

where ω is the angular frequency. $\tilde{R}_{2323}$ is the Fourier function of the tangent shear modulus R_{2323}. $\tilde{g}_1(\omega)$ and $\tilde{g}_2(\omega)$ are the Fourier functions, respectively, of $g_1(t)$ and $g_2(t)$.

In order to have an asymptotic behaviour of the functions $g_i(t)$, these latter are chosen as follows

$$\begin{cases} g_1(t) = a_1 + b_1\,e^{-t/t_1} \\ g_2(t) = a_2 + b_2\,e^{-t/t_2} \end{cases} \tag{25}$$

a_1, b_1, a_2, b_2 are material constants. t_1 and t_2 are relaxation times.

Hence, Eq. (24) becomes

$$\tilde{R}_{2323}(\chi, \omega) = 2A\chi^2\left(\frac{a_1}{i\omega} + \frac{b_1}{i\omega + \frac{1}{t_1}}\right) + 2B\frac{\chi^3(2 + \chi^3)}{1 + 2\chi^3}\left(\frac{a_2}{i\omega} + \frac{b_2}{i\omega + \frac{1}{t_2}}\right) \tag{26}$$

The relaxation times, t_1 and t_2, and the material constants a_1, a_2, b_1 and b_2 are not dependent upon the preload χ. Hence, it is easier to compute these material constants by identifying experimental results of the dynamic modulus unless preload ($\chi = 1$) with Eq. (26) [23].

Relation (26), which characterizes the tangent shear modulus of visco-hyperelastic layers, will be used in calculating the global shear modulus of the multilayer structure which is given by expression (11).

3. Experiment

In this section we present an experimental identification of the multilayer dynamic behaviour in shear. Dynamic shear tests under preload were conducted in an MTS materials testing machine. A specimen presented in Fig. 3, which is called "Shim" and made of a multilayer elastomer-steel, is used. Elastomer layers are made of a synthetic vulcanized rubber. This composite structure is used in brake system for vibro-acoustic isolation. It is stuck on the back of the brake pad. Fig. 4 describes the dynamic test apparatus which is equipped with an electronic measuring system. In the assembly apparatus, presented in Figs. 5–7 we have used an assembly of 12 specimens which is taken into account in calculating the multilayer shear modulus. This is in order to increase the system flexibility at higher frequency. We apply an harmonic shear displacement.

Fig. 8 presents the shear modulus, under various preloads, obtained from dynamic tests and those using the developed model (Eq. (26)). These curves show a hardening phenomenon with preload and frequency. Experimental results are obtained for [0, 200 Hz] frequency range. The preload compression elongation varies from 1 to 0.6.

4. Numerical results

Fig. 8 presents the fitting of the analytical model (26) with the experimental tests of the dynamic modulus according to the frequency at various preloads. The fitting procedure is developed at different preload and it is based on the least square method. We have almost the same values of material constants at each preload. We note a good correlation between the experimental results and the theoretical model (readjusted) with an error lower than 4 percent.

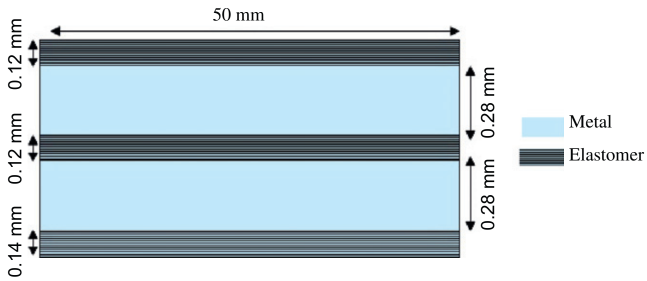

Fig. 3. Structure of a multilayer called "Shim".

Fig. 4. Experimental apparatus for dynamic test on MTS machine (ISMEP, Paris).

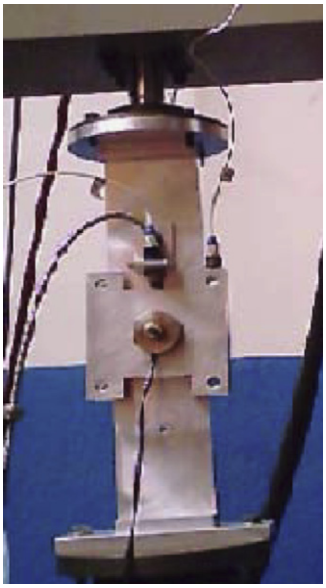

Fig. 5. Assembly apparatus.

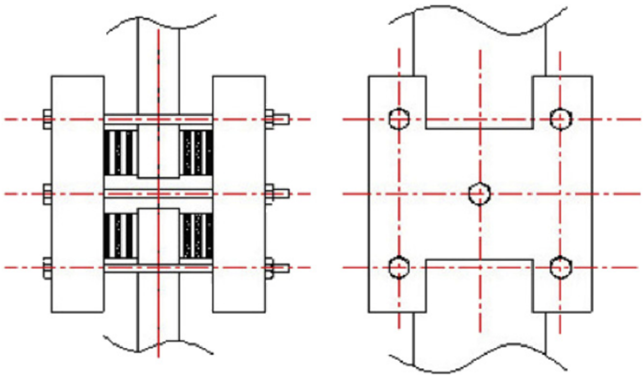

Fig. 6. Attachment unit of the multilayer plates. The multilayer thickness does not respect the real dimension and is dilated.

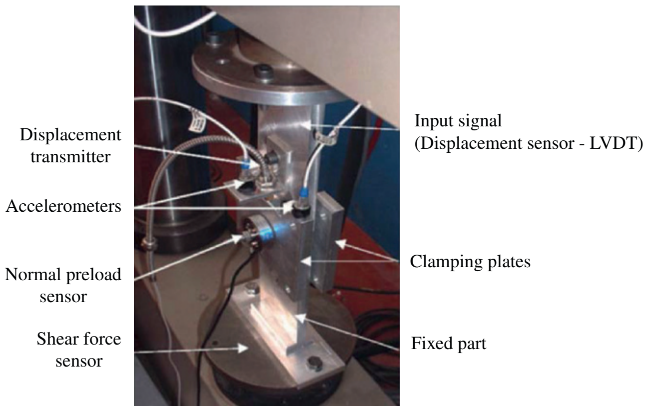

Fig. 7. Assembly apparatus—assembly of the transmitters.

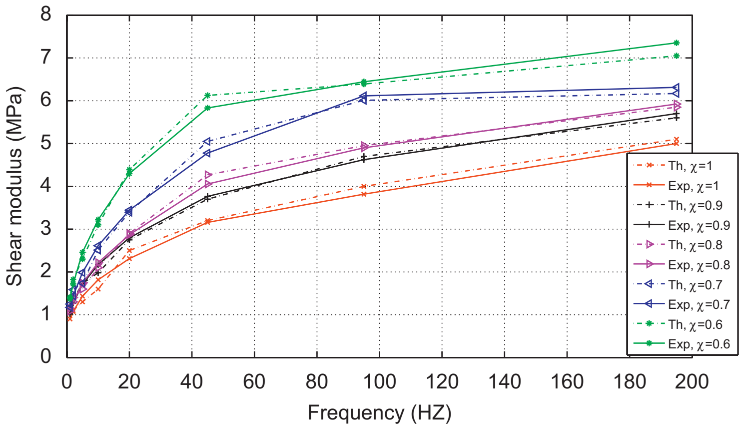

Fig. 8. Dynamic shear modulus fitting: theory and experiences, $A = 299.47$ MPa; $B = 42.8283$ MPa; $a_1 = 51.44$; $a_2 = 11.56$; $b_1 = -37.5996$; $b_2 = -2.4658$; $t_1 = 0.0005$ s; $t_2 = 0.0360$ s.

Table 1
Visco-elastic parameters of the third-order Maxwell model used in Abaqus (Prony series model: $G = G_\infty(1 + \sum_{i=1}^{3} g_i\, e^{-t/\tau_i})$; G is the shear modulus; G_∞ is shear modulus at infinite time; τ_i ($i = 1, 2, 3$) are relaxation times; g_i ($i = 1, 2, 3$) are dimensionless shear modulus.

G_∞ (MPa)	g_1	g_2	g_3	τ_1 (s^{-1})	τ_2 (s^{-1})	τ_3 (s^{-1})
7.7154	0.1333	0.2972	0.3751	0.1260	0.0042	0.0011

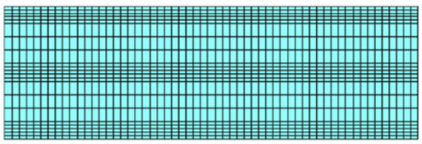

Fig. 9. Mesh of the structure—quadratic element, nine nodes.

4.1. Comparison with finite elements calculations

With an aim of testing the reliability of our model, we simulated the harmonic problem of shearing under preload in the Abaqus code. We chose among the hyperelastic models integrated in Abaqus, that which as well as possible readjusts the experimental behaviour of material in simple traction. We found that the second-order polynomial model described best the behaviour of materials.

The viscoelastic model chosen, in Abaqus, corresponds to the generalized Maxwell model, whose parameters are readjusted by means of creep tests (Table 1).

A plane quadratic element with nine nodes was selected (Fig. 9). A hybrid integration approach was chosen.

We notice according to Fig. 10, a remarkable difference between the experimental results and the results given by Abaqus. This can be explained by the complexity of the model used in Abaqus (hyperélasticity + viscoelasticity + incompressibility) which generates difficult convergence. Moreover, we mention the difficulty of calculation of the hydraustatic pressure in incompressible shear problem using finite elements method.

It is important to underline that if we change parameter material to improve convergence, we will be in an other case of material and we will not have the same material in which we are interested in this work. Indeed, material parameters are identified separately with sufficient precision by tension test for hyperelastic constants and creep tests for viscoelastic ones. In other words, discrepancy between the results of our analytical model

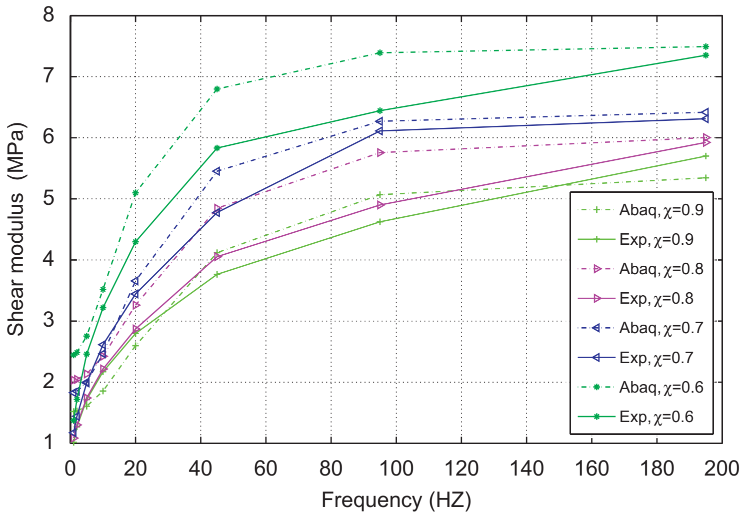

Fig. 10. Comparison between experimental results and Abaqus calculations.

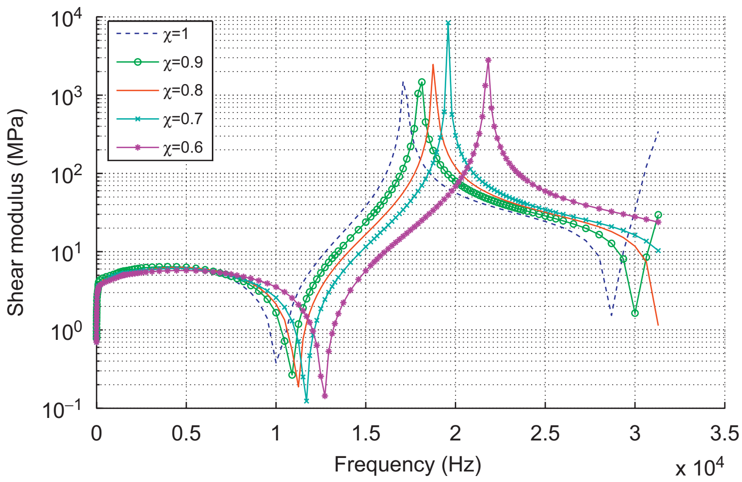

Fig. 11. Shear modulus of a Shim. Analytical model prevision at higher frequency.

and those of ABAQUS is caused by convergence problems and not caused by the parameters used in the ABAQUS model. Convergence problems in Abaqus, are due especially to the nonlinear and complex mathematical approach used for computing visco-hyperelastic structure.

Thus, with lower cost, our model allows us better to apprehend the identification of the dynamic tangent modulus of the multilayer (Eq. (8)).

4.2. *Mass phenomena*

The developed model presents a resonance and an antiresonance phenomena at higher frequencies [10,000, 30,000 Hz] (Fig. 11). These phenomena are due to the mass effect which is generated by metallic layers. A comparison of our model with model corresponding of springs in series is presented in Fig. 12. This latter shows that the simple model of springs in series does not represent these mass phenomena compared to our model. We mention that the advantage of our developed model compared to the model of mass-spring in series which is presented in Fig. 12, is the continuum mechanics aspect. In hence, in Figs. 13 and 14, the displacement

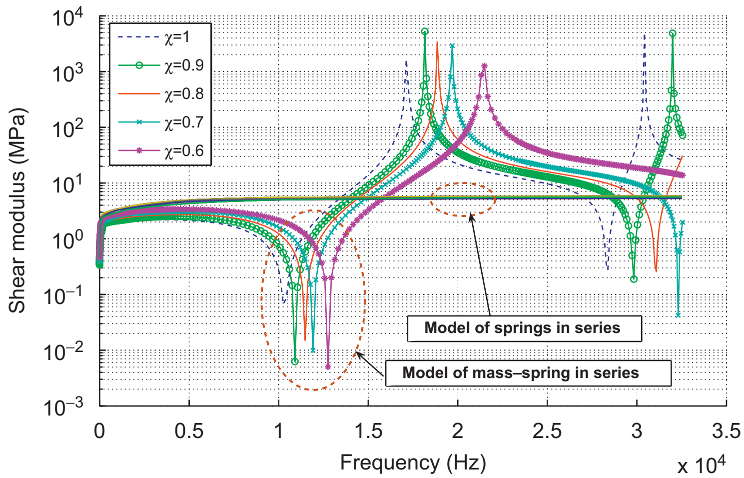

Fig. 12. Model of springs in series and model of springs/masses in series.

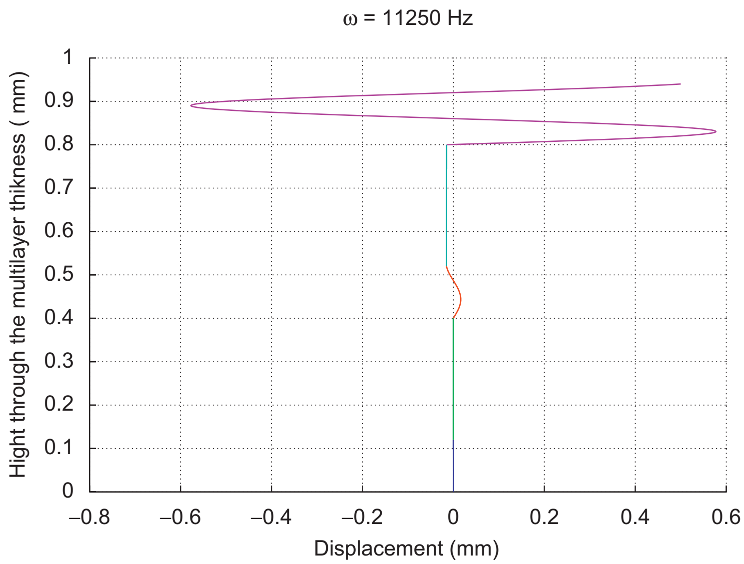

Fig. 13. Displacement solution through the multilayer thickness.

and shear fields are represented through the multilayer thickness. We observe a rigid displacement of the steel layers. In specific case, when the multilayer is composed of two kinds of layers (for example steel with large mass and stiffness and polymer with small mass and stiffness) the proposed model can be approached with discreet mass-spring model (Fig. 12). But, with the proposed model we can study multilayer which is composed of different kinds of materials.

In addition, Fig. 11 presents a structure shear model in the mass effect range and a material shear model elsewhere. This is well observed in Fig. 15 which presents the wavelength of the shear modulus. At lower frequency, the wavelength is grater than the multilayer thickness. In this case, the structure is equivalent to an homogeneous material. In the higher frequency domain ($f > 10,000$ Hz), the wavelength is of a similar value as the multilayer thickness. So in this range of frequency, the structure cannot be considered as homogeneous.

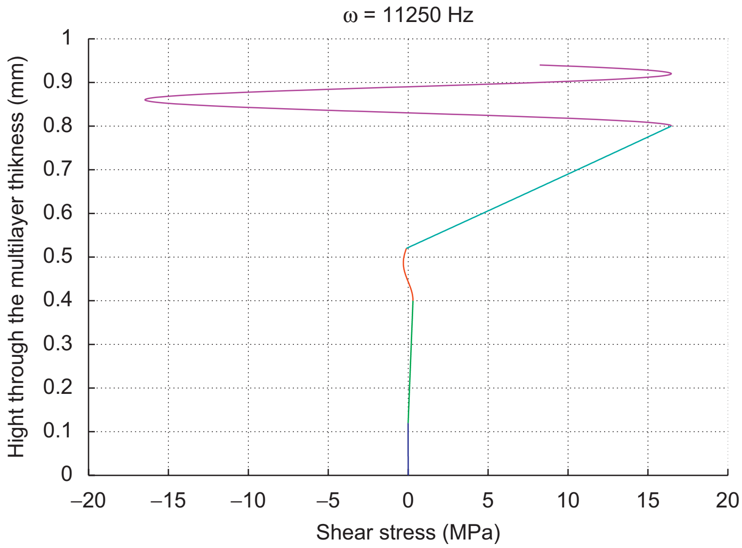

Fig. 14. Shear stress solution through the multilayer thickness.

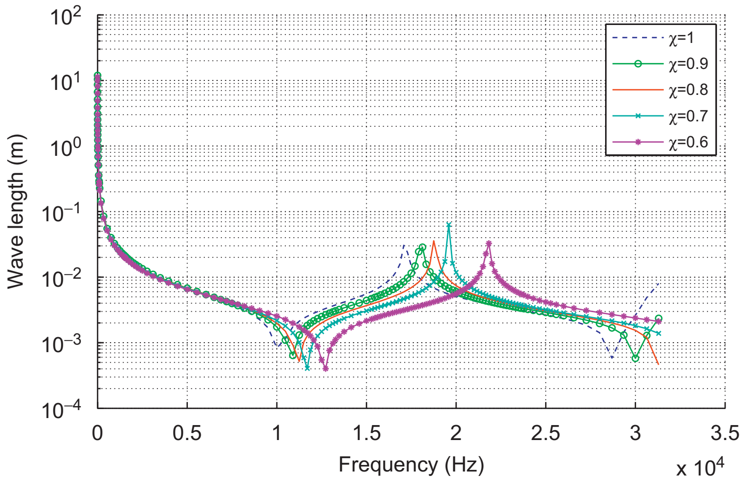

Fig. 15. Wavelength of the shear modulus.

5. Conclusion

In this work, a nonlinear dynamic behaviour of preloaded traditional multilayer plates incorporating visco-hyperelastic materials is investigated. A nonlinear model is proposed to simulate the nonlinear dynamic response. As was shown in the analysis, the analytical method developed herein could provide a nonlinear view of the frequency analysis by taking into account the compression preload and the nonlinear visco-hyperelasticity effects. Verification of the model is performed through a series of dynamic shear tests under various compression preload levels. Numerical results of the developed model show a hardening of the multilayer when increasing the preload level or the frequency. Nonsignificant distinction between theory and experience was observed. However, with lower cost, our model allows us better to apprehend the identification of the dynamic modulus of the multilayer compared to finite element calculations.

At higher frequencies (acoustic domain), we observed mass phenomena whose are due to the metallic layers and cannot be represented by a simple model of springs in series. With the proposed model we can study multilayer which is composed of different kinds of materials. While, the mass-spring model is reliable for multilayer composed of both rigid and flexible materials.

It was well illustrated that developed model herein characterizes an homogeneous material at lower frequencies. In the mass effect range (Higher frequencies), our model characterizes a structure modulus (heterogeneous material).

The prospect of developing this approach within a three-dimensional model will be of great utility for dimensioning complex structures. Thus, it will be of great interest to take into account the interface rubbing. Presently, we are generalizing the presented approach for the case of finite harmonic deformation around preload. This is the case of para-seismic visco-hyperelastic structures.

Acknowledgement

The authors wish to thank BOSCH Breaking Systems for the support that permitted the conduct of this work.

References

[1] A.V. Tobolsky, *Properties and Structure of Polymers*, Wiley, New York, 1960.
[2] J.N. Reddy, *Mechanics of Laminated Composite Plates and Shells. Theory and Analysis*, second ed., CRC Press, Boca Raton, 2004.
[3] J.B. Ever, *Introduction to Composite Materials Design*, Taylor and Francis, Philadelphia, 1988.
[4] W. Swallow, An improved method of damping panel vibrations, British Patent Specification 513171, 1939.
[5] E.M. Kerwin, Damping of flexural waves by a constrained viscoelastic layer, *Journal of the Acoustical Society of America* 31 (1959) 952–962.
[6] E.E. Ungar, E.M. Kerwin Jr., Loss factors of viscoelastic systems in terms of energy concepts, *Journal of the Acoustical Society of America* 34 (1962) 954–957.
[7] R.A. Di Taranto, Theory of vibratory bending for elastic and viscoelastic layered finite-length beams, *Journal of Applied Mechanics—Transactions of the ASME* 32 (1965) 881–886.
[8] R.A. Di Taranto, W. Blasingame, Composite damping of vibrating sandwich beams, *Journal of Applied Mechanics—Transactions of the ASME* (1967) 633–638.
[9] D.J. Mead, S. Markus, Damping sandwich beam with arbitrary boundary conditions, the forced vibration of three layer damped sandwich beam with arbitrary boundary conditions, *Journal of Sound and Vibrations* 10 (1969) 163–175.
[10] T. Fujii, Dynamic response of sandwich beams with an adhesive damping layer (generalized Maxwell model for a viscoelastic adhesive layer), *International Journal of Adhesion and Adhesives* 13 (3) (1993) 201–209.
[11] F. Njilie Adamou, P. Muller, M.T. Gautherin, évaluation de l'amortissement d'une plaque sandwich, acier-polymère-acier, *Mécanique & Industries* 4 (2) (2003) 77–81.
[12] H. Yuh-Chun, H. Shyh-Chin, The frequency response and damping effect of three-layer thin shell with viscoelastic core, *Computers & Structures* 76 (5) (2000) 577–591.
[13] P. Mahmoodi, Structural dampers, *Journal of the Structural Division—ASCE* 95 (1972) 1961–1967.
[14] D.M. Bergamon, R.D. Hanson, Characteristics of viscoelastic damping devices, *Proceeding of the ATC Seminar and Workshop on Base Isolation and Passive Energy Dissipation, Applied Technology Council*, Redwood City, CA, 1986.
[15] H.H. Lee, C.S. Tsai, Analytical model for viscoelastic dampers for seismic mitigation of structures, *International Journal of Computers and Structures* 50 (1994) 111–121.
[16] H.H. Lee, Nonlinear vibration of a multilayer sandwich beam with viscoelastic layers, *Journal of Sound and Vibration* 216 (4) (1998) 601–621.
[17] P. Saad, Modélisation du comportement viscoélastique des élastomères autour d'une précharge (modeling of the nonlinear viscoelastic response of rubber under preload), *Mécanique & Industries* 4 (2003) 133–142 (in French).
[18] P. Saad, Modélisation et identification du comportement nonlinéaire des cales en caoutchouc (Nonlinear Behavior of Rubber Bush, Modeling and Identification), PhD Thesis, Ecole Centrale de Lyon, Lyon, 2003 (in French).
[19] H. Gacem, Comportement visco-hyperélastique des élastomères, viscoélasticié nonlinéaire, application aux multicouches (Visco-hyperelastic Behaviour of Elastomers, Nonlinear Viscoelasticity, Application on Multilayers), PhD Thesis, Pierre et Maris Curie University, Paris 6, December 2007 (in French).
[20] G.A. Holzapfel, *Nonlinear Solid Mechanics*, Wiley, New York, 2000.
[21] T. Beda, Y. Chevalier, Sur le comportement statique et dynamique des élastomères en grandes déformations (on the static and dynamic behaviour of elastomers in large deformations), *Mécanique Industrielle et Matériaux* 50 (5) (1997) 228–231 (in French).
[22] A.N. Gent, A.G. Thomas, Forms for the stored strain energy function for vulcanized rubber, *Journal of Polymer Science* 28 (1958) 625–628.
[23] J.H. Nashif, *Vibration Damping*, Wiley, New York, 1984.